

# ChemComm

Accepted Manuscript



This is an *Accepted Manuscript*, which has been through the Royal Society of Chemistry peer review process and has been accepted for publication.

*Accepted Manuscripts* are published online shortly after acceptance, before technical editing, formatting and proof reading. Using this free service, authors can make their results available to the community, in citable form, before we publish the edited article. We will replace this *Accepted Manuscript* with the edited and formatted *Advance Article* as soon as it is available.

You can find more information about *Accepted Manuscripts* in the [Information for Authors](#).

Please note that technical editing may introduce minor changes to the text and/or graphics, which may alter content. The journal's standard [Terms & Conditions](#) and the [Ethical guidelines](#) still apply. In no event shall the Royal Society of Chemistry be held responsible for any errors or omissions in this *Accepted Manuscript* or any consequences arising from the use of any information it contains.

## COMMUNICATION

Cite this: DOI: 10.1039/x0xx00000x

Received Xth November 2014,

Accepted Xth November 2014

DOI: 10.1039/x0xx00000x

www.rsc.org/ChemComm

A Solution-phase Approach to  $\text{Cd}_3\text{P}_2$  Nanowires: Synthesis and CharacterizationChi Yang,<sup>a,b</sup> Huanhuan Pan,<sup>c</sup> Sheng Liu,<sup>d</sup> Shu Miao,<sup>b</sup> Wen-Hua Zhang,<sup>\*b</sup> Jiansheng Jie,<sup>\*c</sup> Xin Xu,<sup>\*a</sup>

**Single-crystalline  $\text{Cd}_3\text{P}_2$  nanowires (NWs) have been synthesized via solution–liquid–solid (SLS) mechanism. The lengths of the resulting nanowires can be effectively tuned in the range of 180 nm and 5  $\mu\text{m}$ , and the photodetectors made of the  $\text{Cd}_3\text{P}_2$  nanowires exhibited a pronounced photoresponse with high stability and reproducibility.**

One-dimensional semiconductor nanowires (NWs) have raised considerable research interests due to their high aspect ratio and dimensional-dependent physical and electronic properties. They exhibit two quantum confined directions, while provide a natural pathway for charge carrier transport along the unconfined direction. This unique feature makes them suitable as building blocks of electronic devices. For instance, in photovoltaic cells, high-aspect-ratio nanowires have the potential for enhancement of electron transport in contrast to nanoparticles (NPs), thereby leading to superior device performance.<sup>1,2</sup> Moreover, it is pivotal to control the synthesis of semiconductor nanowires for exploiting their applications, such as photodetectors.<sup>3–7</sup>

Cadmium phosphide ( $\text{Cd}_3\text{P}_2$ ) is featured of a small direct band gap (0.55 eV), a large exciton Bohr radius (18 nm), a relatively high dielectric constant (5.8), and a small effective mass of the electron.<sup>8–10</sup> A number of papers have reported the synthesis of  $\text{Cd}_3\text{P}_2$  nanostructures and their potential applications in optoelectronics.<sup>11–14</sup> However, the synthesis of  $\text{Cd}_3\text{P}_2$  NWs has been rarely reported to date. To the best of our knowledge, the only one report on  $\text{Cd}_3\text{P}_2$  nanowires synthesis was most recently described by Fan et al., wherein  $\text{Cd}_3\text{P}_2$  NWs were prepared using InP as P precursor and Cd foil as the source of Cd at temperature as high as 900 °C via a chemical vapor deposition (CVD) process<sup>15</sup>.

Currently, several efficient approaches have been developed to grow high-quality semiconductor NWs, e.g., nanochannel template growth,<sup>16–18</sup> vapor-liquid-solid (VLS) growth,<sup>19–22</sup> supercritical-fluid-liquid-solid (SFLS) growth,<sup>23</sup> and SLS growth.<sup>24,25</sup> Among them, the solution approaches seeded by low-melt metal catalyst offer appealing properties, including relatively low growth temperatures (generally < 400 °C),<sup>26,27</sup> high-crystalline structure, and tunable length. However, synthesis of nanowires by solution

approach is limited by growth solvents as well as precursors. Thus the semiconductor nanowires prepared by solution catalytic approach are much fewer than those via VLS growth, which is usually performed at high temperatures (e.g., > 700 °C). In this work, we exploited the SLS approach to grow single-crystalline  $\text{Cd}_3\text{P}_2$  nanowires using Bi nanoparticles as catalysts at temperature of only 290 °C. The length of the resulting nanowires can be tuned in the range of 180 nm ~ 5  $\mu\text{m}$  by varying the ratio of Bi NPs/  $\text{Cd}_3\text{P}_2$  precursors while their diameter was kept basically unchanged at ~ 16 nm. Experiments further show that the  $\text{Cd}_3\text{P}_2$  nanowires exhibit absorption spanning visible-to-near-infrared range, and the photodetectors made of these nanowires shows a pronounced photoresponse with high stability and reproducibility, and their sensitivity enhances with the decrease of light wavelength.

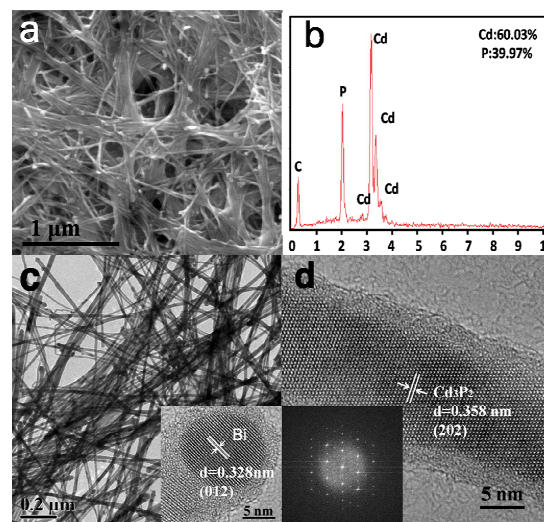


**Fig. 1.** a) SEM image, b) EDX spectrum and c) TEM image of an ensemble of randomly aligned  $\text{Cd}_3\text{P}_2$  nanowires. (Inset shows the HRTEM image of a Bi NP at the wire tip). d) HRTEM image of a part of the  $\text{Cd}_3\text{P}_2$  nanowire. (Inset shows the FFT of the image). These images have obtained in the  $\text{Cd}_3\text{P}_2$  nanowires prepared with Cd/P molar ratio of 6/1.

Fig. 1a shows the scanning electron microscopy (SEM) images of the ensemble of randomly aligned  $\text{Cd}_3\text{P}_2$  nanowires that were

prepared with Cd/P molar ratio of 6/1 in the synthesis precursor. The nanowires show lengths up to 5  $\mu\text{m}$  with relative uniform diameter. EDX linked with SEM was performed to reveal the chemical composition of the  $\text{Cd}_3\text{P}_2$  NWs, as presented in Fig. 1b. The atomic ratio of Cd/P measured in the products is very close to the ideal composition of 3/2 for  $\text{Cd}_3\text{P}_2$  materials, indicative of the formation of well stoichiometric product. The TEM image in Fig. 1c displays smooth nanowires with a mean diameter of  $\sim 15.9$  nm, which correlates to the size of monodisperse Bi-nanoparticle catalysts ( $13.3 \text{ nm} \pm 1.2$ ). A Bi catalyst nanoparticle attached to the wire tip was clearly revealed: the catalyst nanoparticle appears darker in the image because of Z contrast:  $Z_{\text{Bi}} > Z_{\text{Cd}} > Z_{\text{P}}$  as shown in the inset of Fig. 1c. Furthermore, it reveals a d-spacing of 0.328 nm, as the (012) plane of rhombohedral Bi. To further study the growth of the  $\text{Cd}_3\text{P}_2$  nanowires, the microstructures of the  $\text{Cd}_3\text{P}_2$  nanowires were analyzed by high-resolution TEM (HRTEM). Fig. 1d shows a single  $\text{Cd}_3\text{P}_2$  nanowire with a d-spacing of 0.358 nm, well-matched the (202) plane of tetragonal  $\text{Cd}_3\text{P}_2$ . These results confirm that the  $\text{Cd}_3\text{P}_2$  nanowires were formed via the SLS mechanism,<sup>24</sup> and the growth direction of the  $\text{Cd}_3\text{P}_2$  nanowires is perpendicular to the (202) lattice plane. The fast Fourier transform (FFT) of the image (inset of Fig. 1d) further confirms this preferential growth direction of the nanowires. The sharp diffraction maxima in the FFT demonstrate the single crystalline nature of the crystal. More HRTEM images of a number of individual  $\text{Cd}_3\text{P}_2$  NWs are shown in Fig. S1, ESI†, confirming this conclusion.

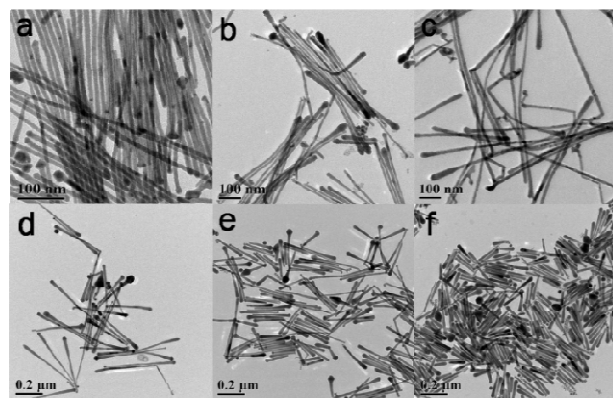


**Fig. 2.** TEM images of the  $\text{Cd}_3\text{P}_2$  NWs synthesized with different Cd/P molar ratios of (a) 4/1, (b) 8/1, (c) 10/1 and different amount of (d) 2.0  $\mu\text{mol}$ , (e) 4.0  $\mu\text{mol}$ , and (f) 6.0  $\mu\text{mol}$  of Bi nanoparticle catalysts.

The influence of precursors was studied to optimize the  $\text{Cd}_3\text{P}_2$  nanowire growth. Fig. 2 shows the TEM images of the  $\text{Cd}_3\text{P}_2$  nanowires prepared with the different ratios of Cd/P. It is apparent that the ratios of the precursors play an important role in affecting the quality of the resulting nanowires. Fig. 2 shows that high quality  $\text{Cd}_3\text{P}_2$  nanowires with smooth surface and relative uniform diameters can be obtained when Cd/P ratios were at 4/1 (Fig. 2a) and 6/1 (Fig.

1c). As Cd/P ratios continued to increase, the NWs would be curve or dendritic as shown in Fig. 2b (Cd/P=8:1) and Fig. 2c (Cd/P=10:1). It is hence appropriate to keep the Cd/P ratio in the range of 4/1~6/1 to obtain high quality  $\text{Cd}_3\text{P}_2$  nanowires in this study. Further study on  $\text{Cd}_3\text{P}_2$  nanowires were therefore focused on the sample prepared with Cd/P ratio of 6/1. Interestingly, further study show that the lengths of the  $\text{Cd}_3\text{P}_2$  nanowires can be effectively tuned by varying the amount of Bi nanoparticle catalysts used in the reaction: Nanowires with length over 5  $\mu\text{m}$  can be obtained under condition that 1.2  $\mu\text{mol}$  of Bi nanoparticle catalysts was involved in the reaction (shown in Fig. 1). However, the length of the  $\text{Cd}_3\text{P}_2$  nanowires can be rapidly reduced to  $\sim 450$  nm if the amount of Bi NP catalyst was increased to 2.0  $\mu\text{mol}$  (Fig. 2d), and further decreased to  $\sim 230$  nm (Fig. 2e) and 180 nm (Fig. 2f) when 4.0  $\mu\text{mol}$  and 6.0  $\mu\text{mol}$  of Bi NP catalysts were used, respectively. This is in line with the fact that, a decrease of the amount of Bi nanoparticle catalysts employed in the synthesis generally led to an increase of nanowire lengths for the SLS grown nanowires.<sup>28</sup> In addition we have attempted to tune the diameters of the  $\text{Cd}_3\text{P}_2$  nanowires by varying the sizes of Bi catalysts. However, it was found that all of the resulting  $\text{Cd}_3\text{P}_2$  shows similar diameters in the range of 13 nm to 17 nm shown in (Fig. S2, ESI†).

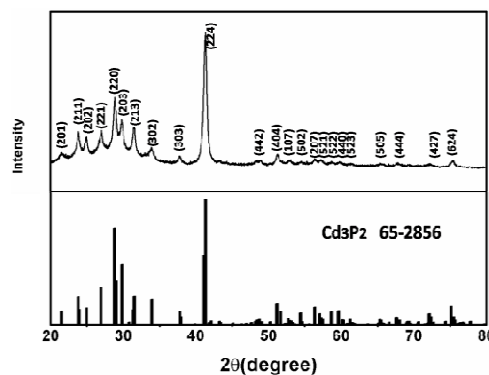


**Fig. 3.** XRD patterns for the  $\text{Cd}_3\text{P}_2$  nanowires.

Fig. 3 shows a typical XRD pattern for the  $\text{Cd}_3\text{P}_2$  nanowires with length of  $\sim 5$   $\mu\text{m}$ . The peak broadening is characteristic of a material at nanoscale. The NWs exhibits a number of well-resolved reflection peaks that can be indexed to the (221), (220), (203), (213) and (224) planes of  $\text{Cd}_3\text{P}_2$  structure, respectively (JCPDS No. 65-2856). Therefore, pure phase  $\text{Cd}_3\text{P}_2$  nanowires were successfully synthesized with high-crystalline structures by the solution-solid-liquid mechanism via the Bi NP catalytic role.

The UV/Vis/NIR absorbance spectra of the colloidal  $\text{Cd}_3\text{P}_2$  nanowires suspensions were measured to study the optical properties. The  $\text{Cd}_3\text{P}_2$  nanowires absorbed light across the near-infrared to the entire visible spectrum (Fig. S3, ESI†), thus making suspensions

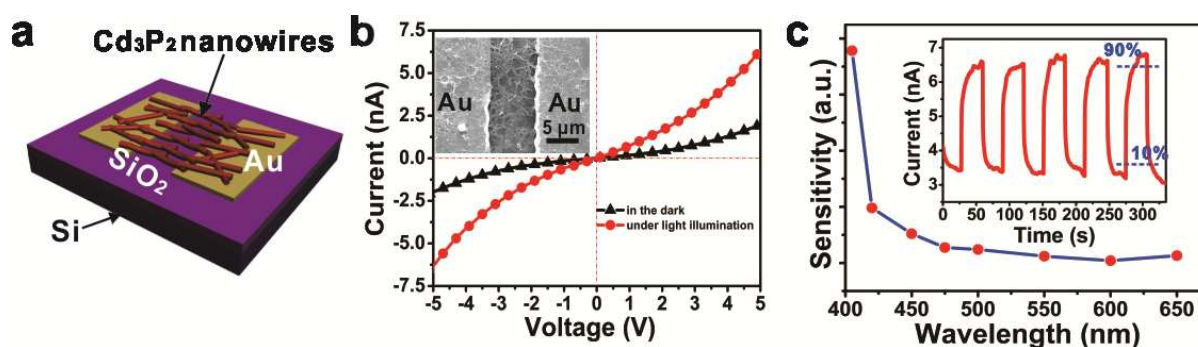


**Fig. 4.** (a) Schematic illustration of the photodetector fabricated from the Cd<sub>3</sub>P<sub>2</sub> nanowire network. (b) *I*-*V* curves of the photodetector measured in the dark and under light illumination (405 nm, 7.5 mw/cm<sup>2</sup>), respectively. Inset shows the SEM image of a typical device. (c) Wavelength-dependent sensitivity of the photodetector. Photoresponse of the photodetector to pulsed light is shown in the inset.

brownish black color. The indirect optical band gap (inset of Fig. S3, ESI†) of the typical Cd<sub>3</sub>P<sub>2</sub> nanowires were determined at 0.78 eV, which is a little larger than that of the bulk materials, probably attributed to size quantum effect or surface effect. To study the optoelectronic properties of the Cd<sub>3</sub>P<sub>2</sub> nanowires, the transient photocurrent response was first tested by a photoelectrochemical cell. A Cd<sub>3</sub>P<sub>2</sub> nanowire film was prepared by spray-casting a nanowire suspension in hexane onto FTO substrate. The film was then annealed at 150 °C for subsequent measurement under illumination with a Xenon lamp. As shown in Fig. S4, ESI†, when tuning on the light, the current increased quickly. Oppositely, the current decreased when the light tuned off, indicative of their sensitivity to light irradiation. Moreover, when the potential was enlarged, the response would be increased. This clearly demonstrates n-type semiconducting behavior for the resulting Cd<sub>3</sub>P<sub>2</sub> nanowires in this study.

To gain more insight into the optoelectronic properties of the Cd<sub>3</sub>P<sub>2</sub> nanowires, photodetectors based on the Cd<sub>3</sub>P<sub>2</sub> nanowire network were fabricated by directly drop-casting the nanowires on pre-prepared Au electrode pairs on SiO<sub>2</sub> (300 nm)/Si substrate. Schematic illustration and SEM image of the photodetector are shown in Fig. 4a and inset of Fig. 4b, respectively. From the current versus voltage (*I*-*V*) curves of a typical device measured in the dark condition and under light illumination (405 nm, 7.5 mw/cm<sup>2</sup>) (Fig. 4b), one can see that the photodetector shows a pronounced photoresponse. The photocurrent from Cd<sub>3</sub>P<sub>2</sub> NWs in this work is significantly lower than that of PCBAME/Cd<sub>3</sub>P<sub>2</sub> hybrid NWs prepared via CVD at high temperature.<sup>15</sup> It is known that the organic oleic acid (OA) are indispensable to the growth of Cd<sub>3</sub>P<sub>2</sub> NWs in this study by colloidal chemistry, while they can form an insulating layer to suppress injection or extraction of charge carriers from the NWs. We have conducted ligand exchange to improve the conductivity of the NWs by removing the insulating OA layer with hydrazine hydrate.<sup>29</sup> However, it is impossible to completely remove the organic ligand by such ligand exchange strategy. Therefore, the device performance of the colloidal nanowires is still worse than that

of CVD-grown bare nanowires. Additionally, the device can be reversibly switched between low- and high-resistivity states when the light is switched on and off repeatedly (inset of Fig. 4c), revealing the high stability and reproducibility of the photodetector. The response time and recovery time, defined as the time intervals from 10% to 90% of the difference between maximum and minimum current, are deduced to be 7.2 s and 4.9 s, respectively. Fig. 4c shows the wavelength-dependent sensitivity of the photodetector. Notably, the device exhibits high sensitivity to the short-wavelength light, and the sensitivity enhances with the decrease of light wavelength.

In summary, high quality Cd<sub>3</sub>P<sub>2</sub> nanowires have been synthesized using Bi nanoparticles as seeded catalyst via SLS mechanism at only 290 °C. The lengths of nanowires can be varied in the range of 180 nm ~ 5 μm by changing the synthetic parameters. Experiments demonstrate that the as-prepared Cd<sub>3</sub>P<sub>2</sub> NWs are single-crystalline structured materials with light absorption across visible-to-near-infrared ranges. Photoelectrochemical measurement reveals they are n-type semiconductor and are sensitive to light irradiation. Moreover, photodetectors made of these nanowires exhibit the high sensitivity to short-wavelength light, confirming the great potential of Cd<sub>3</sub>P<sub>2</sub> nanowires in high-performance optoelectronic devices.

This research was supported by the National Science Foundation of China (No. 11179037, 51172151 and 51402242).

## Note and references

- CAS Key Laboratory of Materials for Energy Conversion, Department of Materials Science and Engineering, University of Science and Technology of China, Hefei 230026, China
- State Key Laboratory of Catalysis, Dalian Institute of Chemical Physics, Chinese Academy of Sciences, 457 Zhongshan Road, Dalian 116023, China
- Institute of Functional Nano & Soft Materials (FUNSOM), Soochow University, Suzhou 215123, China
- School of Chemistry and Chemical Engineering, Southwest University, Chongqing 400715, China



Electronic supplementary information (ESI) available: detailed experimental, TEM, UV-Visible absorption spectra and Transient photocurrent response. See DOI: 10.1039/x0xx00000x /

- 1 S. Liu, X. Y. Guo, M. R. Li, W. H. Zhang, X. Y. Liu, C. Li, *Angew. Chem. Int. Ed.*, 2011, **50**, 12050.
- 2 J. Wallentin, N. Anttu, D. Asoli, M. Huffman, I. Aberg, M.T. Borgstrom, *Science*, 2013, **339**, 1057.
- 3 D. J. Xue, J. H. Tan, J. S. Hu, W. P. Hu, Y. G. Guo, L. Y. Wan, *Adv. Mater.*, 2012, **24**, 4528.
- 4 S. Bai, W. W. Wu, Y. Qin, N. Y. Cui, D. J. Bayerl, X. D. Wang, *Adv. Funct. Mater.*, 2011, **21**, 4464.
- 5 J. J. Wang, F. F. Cao, L. Jiang, Y. G. Guo, W. P. Hu, L. Y. Wan, *J. Am. Chem. Soc.*, 2009, **131**, 15602.
- 6 D. S. Wang, C. H. Hao, W. Zheng, Q. Peng, T. H. Wang, Z. M. Liao, D. P. Yu, Y. D. Li, *Adv. Mater.*, 2008, **2**, 2628.
- 7 X. Fan, X. M. Meng, X. H. Zhang, M. L. Zhang, J. S. Jie, W. J. Zhang, C. S. Lee, S. T. Lee, *J. Phys. Chem. C.*, 2008, **113**, 834.
- 8 R. G. Xie, J. X. Zhang, F. Zhao, W. S. Yang, X. G. Peng, *Chem. Mater.*, 2010, **22**, 3820.
- 9 S. D. Miao, S. G. Hickey, B. Rellinghaus, C. Waurisch, A. Eychmüller, *J. Am. Chem. Soc.*, 2010, **132**, 5613.
- 10 O. Wilfried-Solo, X. Shu, D. Fabien, N. Céline, C. Bruno, *Angew. Chem. Int. Ed.*, 2012, **51**, 738.
- 11 A. M. Hermann, A. Madan, M. W. Wanlass, V. Badri, R. Ahrenkiel, S. Morrison, *Sol. Energy. Mater. Sol. Cells.*, 2004, **82**, 241.
- 12 M. Bhushan, A. Catalano, *Appl. Phys. Lett.*, 1981, **38**, 39.
- 13 H. Weller, *Adv. Mater.*, 1993, **5**, 88.
- 14 H. Weller, *Angew. Chem. Int. Ed.*, 1993, **32**, 41.
- 15 G. Chen, B. Liang, X. Liu, Z. Liu, G. Yu, X. M. Xie, T. Luo, *ACS Nano.*, 2014, **8**, 787.
- 16 D. S. Xu, D. P. Chen, Y. J. Xu, X. S. Shi, G. L. Guo, L. L. Gui, *Pure. Appl. Chem.*, 2000, **72**, 127.
- 17 B. B. Lakshmi, P. K. Dorhout, C. R. Martin, *Chem. Mater.*, 1997, **9**, 857.
- 18 G. Che, B. B. Lakshmi, C. R. Martin, E. R. Fisher, *Chem. Mater.*, 1998, **10**, 260.
- 19 R. S. Wagner, W. C. Ellis, *Appl. Phys. Lett.*, 1964, **4**, 89.
- 20 M. Yazawa, M. Koguchi, K. Hiruma, *Appl. Phys. Lett.*, 1991, **58**, 1080.
- 21 M. Yazawa, M. Koguchi, A. Muto, M. Ozawa, K. Hiruma, *Appl. Phys. Lett.*, 1992, **61**, 2051.
- 22 A. M. Morales, C. M. Lieber, *Science*, 1998, **279**, 208.
- 23 (a) J. D. Holmes, K. P. Johnsto, R. C. Doty, B. A. Korgel, *Science.*, 2000, **287**, 1471; (b) G. Colins, M. Kolesnik, V. Krstic, J. D. Holmes, *Chem. Mater.*, 2010, **22**, 5235.
- 24 T. J. Trentler, K. M. Hickman, S. C. Goel, A. M. Viano, P. C. Gibbons, W. E. Buhro, *Science*, 1995, **270**, 1791.
- 25 F. D. Wang, A. G. Dong, J. W. Sun, R. Tang, H. Yu, W. E. Buhro, *Inorg. Chem.*, 2006, **45**, 7511.
- 26 W. E. Buhro, K. M. Hickman, T. J. Trentler, *Adv. Mater.*, 1996, **8**, 685.
- 27 J. W. Grebinski, K. L. Richter, J. Zhang, T. H. KoselH, M. Kuno, *J. Phys. Chem. B.*, 2004, **108**, 9745.
- 28 F. D. Wang, W. E. Buhro, *Small*, 2010, **6**, 573.
- 29 F. J. Fan, B. Yu, Y. X. Wang, Y. L. Zhu, X. J. Liu, S. H. Yu, Z. F. Ren, *J. Am. Chem. Soc.*, 2011, **133**, 15910.

Graphic for table of contents

